Schwannoma of the extremities: the role of PET in preoperative planning

Adel Refaat Ahmed[1], Hideomi Watanabe[1], Jun Aoki[2], Tetsuya Shinozaki[1], Kenji Takagishi[1]

[1] Department of Orthopedic Surgery, Gunma University Faculty of Medicine, 3-39-15 Showa, Maebashi, Gunma 371-8511, Japan
[2] Department of Diagnostic Radiology, Gunma University Faculty of Medicine, Maebashi, Gunma, Japan

Received 17 March and in revised form 28 May 2001 / Published online: 2 August 2001

Abstract. The aim of this study was to determine the relative utility of various preoperative diagnostic imaging modalities for the evaluation of benign schwannoma, including positron emission tomography (PET) utilising fluorine-18 fluoro-2-deoxy-D-glucose (FDG) and fluorine-18 α-methyl tyrosine (FMT), computed tomography (CT), magnetic resonance imaging (MRI) and digital subtraction angiography (DSA). We retrospectively reviewed imaging findings in 22 patients with 25 histopathologically documented benign schwannomas of the extremities. Pre-operative imaging included: FDG-PET (*n*=22), FMT-PET (*n*=17), MRI (*n*=25), CT (*n*=16) and DSA (*n*=17). All 22 lesions examined by PET with FDG and/or FMT showed accumulation. The standardised uptake values (SUVs) for FDG-PET for the 22 examined tumours ranged from 0.33 to 3.7, and eight of them (36.4%) were assessed as malignant on the basis of their uptake. The SUVs for FMT ranged from 0.44 to 1.47, and 15 out of the 17 evaluated (88.2%) showed values indicating the tumour to be benign. CT demonstrated variable attenuation and contrast enhancement. MRI signal characteristics were relatively consistent: iso-signal or darker than skeletal muscle on T1-weighted and iso-signal or brighter than subcutaneous fat on T2-weighted images. The venous tumour staining depicted on DSA was found to be significantly correlated with FDG accumulation. All tumours but one were treated by surgical enucleation. One tumour suspected to be malignant on the basis of imaging findings was treated with primary wide resection. Although CT, MRI and PET studies are all useful for the detection and localisation of schwannoma, our findings suggest that, among the imaging modalities studied, FMT-PET may be the most reliable technique for the differentiation of benign schwannoma from malignancy.

Hideomi Watanabe (✉)
Department of Orthopedic Surgery,
Gunma University Faculty of Medicine,
3-39-15 Showa, Maebashi, Gunma 371-8511, Japan
e-mail: hidewa@showa.gunma-u.ac.jp
Tel.: +81-27-2208261, Fax: +81-27-2208275

Keywords: Schwannoma – Diagnosis – Positron emission tomography

Eur J Nucl Med (2001) 28:1541–1551
DOI 10.1007/s002590100584

Introduction

Benign schwannoma, also known as neurilemoma, neurinoma and perineural fibroblastoma, is the most common tumour of the peripheral nervous system [1]. Although most schwannomas are solitary, recently patients with multiple lesions have been reported [2]. Schwannoma is an encapsulated tumour arising from the nerve sheath. The encapsulation and the presence of two components, a highly ordered cellular component (Antoni A area) and a looser myxoid component (Antoni B area), distinguish schwannoma from neurofibroma. Schwannoma occurs at all ages but is most commonly found in individuals between 20 and 50 years old [1]. It has a predilection for the head, neck and flexor surfaces of the upper and lower extremities, with the peroneal and ulnar nerves most commonly affected in the limbs [3].

In clinical practice, the evaluation of many musculoskeletal masses remains a diagnostic dilemma. While computed tomography (CT) and magnetic resonance imaging (MRI) are excellent tools for assessing anatomical details, including tumour location, extent and inhomogeneity, they are unreliable both as indicators of the extent of active tumour cell distribution and in distinguishing between malignant and benign lesions [4]. These limitations hinder preoperative planning and biopsy site selection for possible malignant tumours. Resection of schwannomas must be performed carefully, otherwise important neurological elements may be endangered. Preoperative diagnosis of schwannomas must be as accurate as possible in order to facilitate such careful excision with enucleation, and also to avoid inappropriate surgery for other possible malignant lesions [5].

The radiological findings in cases of schwannoma have previously been reported by many investigators. However, few have reported on the MRI features of this tumour [6, 7], and to the best of our knowledge no one has reported a specialised study on positron emission tomography (PET) using fluorine-18 fluoro-2-deoxy-D-glucose (FDG) and fluorine-18 α-methyl tyrosine (FMT) in peripheral schwannomas. The glucose analogue, FDG, is widely used to evaluate various tumours [8]. Several investigators have reported observations with FDG-PET imaging of musculoskeletal tumours, demonstrating a relationship between FDG uptake and histopathological grade [9, 10, 11]. It has also been suggested that FDG-PET might be a useful adjunct in the preoperative evaluation of soft tissue tumours [12, 13]. However, the ability of FDG-PET to differentiate some benign tumours like schwannoma from malignant tumours has been shown to be limited [13]. Recently, FMT was developed as a tumour-detecting amino acid tracer for PET imaging [14]. In a recent clinical trial, it was clearly demonstrated that FMT-PET is of potential clinical value for the detection of brain tumours [15]. We recently demonstrated that FMT is superior to FDG in the differentiation of malignancies from benign lesions [16]. The present study compared the efficacy of FDG- and FMT-PET for the evaluation of schwannomas, and correlated the imaging characteristics on PET with those on CT, MRI and digital subtraction angiography (DSA). Interestingly, high uptake of FDG by some schwannomas has recently been noted by other investigators [17] and was also found in this study.

Materials and methods

Patients. Between December 1997 and December 1999, 26 patients with 29 peripheral nerve sheath tumours were operated on in our institute. Four patients (with four lesions) were excluded as their histological diagnoses were two neurofibromas, one malignant schwannoma and one malignant peripheral nerve sheath tumour. The remaining 22 patients (12 males and 10 females, aged 24–73 years with a mean of 48.1 years) with 25 (preoperatively suspected and postoperatively histopathologically documented) schwannomas of the extremities formed the study group (Table 1). Our patients were studied in a prospective manner to assess the value of various preoperative diagnostic modalities, namely CT, MRI, DSA and PET utilising FDG and FMT. Twelve lesions were located in the upper extremities and 13 in the lower extremities. One patient had developed schwannomas at three different sites (lesions number 10–12) of the right upper limb (anterior aspect of delto-pectoral area, medial aspect of the arm and anterior aspect of the forearm), while another patient had two tumours (lesions number 18 and 19) originating from the tibial nerve at the left knee and the posterior tibial nerve at the right ankle. Twenty tumours presented with local pain and/or tenderness at the tumour site (80%), and ten caused paraesthesia (40%). All tumours but one produced local swelling (96%). None of the patients had motor deficits, and 19 tumours (76%) elicited a positive Tinel's sign. All tumours were examined by MRI, 16 by CT, 17 by DSA, 22 by FDG-PET and 17 by FMT-PET.

The local ethics committee (Gunma University) approved the study, and each individual participating in the PET study gave his or her informed consent.

Evaluation of CT, MRI and DSA. CT was performed to evaluate tumour homogeneity, attenuation and enhancement characteristics. MRI studies were performed using superconducting magnetic systems and the multislice conventional spin-echo technique. T1-weighted images (TR/TE: 550–600/25–40) and T2-weighted images (TR/TE: 1700–2000/70–80) were always obtained. The signal intensity and extent of the tumour, as well as its relationship to the adjacent structures, were determined. Gadolinium was used as a contrast medium to verify enhancement of the lesion in 22 tumours. The lesions were evaluated angiographically according to Abramowitz et al. [18]. Briefly, the degree of vascularity (mild, moderate or severe), the presence or absence of scattered small puddles of contrast medium (seen in the mid-arterial, capillary and venous phases), the presence or absence of multiple feeding vessels, arteriovenous shunting and vascular encasement were examined. Furthermore, the presence or absence of venous tumour staining was evaluated.

PET studies. PET studies were performed as described elsewhere [16]. FDG was synthesised as described previously [13, 16]; FMT was produced in our cyclotron facility using the method developed by Tomiyoshi et al. [14]. Prior to the PET study, patients fasted for at least 4 h, at which time normal glucose levels were confirmed by clinical laboratory tests [19, 20]. PET studies were performed using a whole-body PET scanner, SET2400W (Shimazu Coop, Tokyo, Japan) with a 59.5-cm transaxial field of view and a 20-cm axial field of view, which produced 63 image planes spaced 3.125 mm apart. Transaxial resolution at the centre of the field was 4.2 mm.

A static image, using a simultaneous emission-transmission method with a rotating external source (370 MBq $^{68}Ge/^{68}Ga$ at installation) [21], was initiated 40 min after the injection of 185–350 MBq FMT or FDG. The software was set to provide an 8-min acquisition per bed position and 1–2 bed positions. Attenuation-corrected transaxial images with FMT and FDG were produced by an ordered subset expectation maximisation (OS-EM) iterative algorithm (an ordered subset of 16 with 1 iteration). Images were reconstructed into 128×128 matrices with pixel dimensions of 4.0 mm in-plane and 3.125 mm axially. Using transaxial images, coronal images with a 9.8-mm slice thickness were produced for visual interpretation.

PET data analysis. All PET images were prospectively interpreted in routine hard-copy consensus visual review by an experienced radiologist and an orthopedic surgeon, and were compared with CT scans, MR images, and DSA findings.

For the semiquantitative analysis, functional images of the standardised uptake value (SUV) were produced using attenuation-corrected transaxial images, injected doses of FMT and FDG, patient's body weight, and the cross-calibration factor between PET and dose calibration. SUV was defined as follows:

$$\mathrm{SUV} = \frac{\mathrm{Radioactive\,concentration\,in\,the\,tumour\,(MBq/g)}}{\mathrm{Injected\,dose\,(MBq)/patient's\,body\,weight\,(g)}}.$$

Regions of interests (ROIs) 1 cm in diameter were drawn on the SUV images over the area corresponding to the tumour, which included the site of maximal FMT or FDG uptake. ROI analysis was conducted by a nuclear radiologist with the aid of corresponding CT scans and MR images. The average SUV in the ROI was defined as the tumour uptake of FMT and FDG.

Table 1. Pre- and postoperative clinical data

Lesion	Age	Sex	Site	Nerve	Size (cm)	Pre-operative				Surgery	Postoperative		
						Pain	Tinel's sign	Swelling	Paraesthesia		Pain	Tinel's sign	Paraesthesia
1	45	M	Arm	Median	5×4×3.5	+	–	+	–	Enucleation	–	–	–
2	59	F	Foot	Motor br.	1.5×1×2	+	–	+	–	Enucleation	–	–	–
3	51	M	Knee	Peroneal	2×3×2	+	+	+	–	Enucleation	–	–	+
4	27	M	Forearm	Median	2×2×2	+	+	+	+	Enucleation	–	–	–
5	24	F	Shoulder	Brachial pl.	3×4.4×2	+	+	+	+	Enucleation	–	–	–
6	39	F	Forearm	Ulnar	5×6×4	+	+	+	–	Enucleation	–	–	–
7	27	F	Shoulder	Sensory br.	2×3×2	–	+	+	+	Enucleation	–	–	+
8	40	F	Arm	Median	2×2×3	–	+	+	–	Enucleation	–	–	–
9	50	M	Thigh	Sciatic	4.5×4×3	+	+	+	–	Enucleation	–	–	–
10	59	F	Arm	Sensory br.	2×2×2	+	+	+	–	Enucleation	–	–	–
11	59	F	Arm	Sensory br.	5×3×4	+	+	+	–	Enucleation	–	–	–
12	59	F	Forearm	Sensory br.	4×3×4	+	+	+	–	Enucleation	–	–	–
13	53	M	Wrist	Sensory br.	2×2×3	–	+	+	+	Enucleation	–	+	+
14	50	F	Thigh	Sensory br.	8×5×4	–	–	+	–	Wide resection	–	–	+
15	57	M	Inguinal	Sensory br.	4×5×3	+	+	+	–	Enucleation	–	–	–
16	64	F	Leg	Post. tib.	3×2.5×3	–	+	+	–	Enucleation	–	–	–
17	40	M	Shoulder	Brachial pl.	2×2×2	+	+	–	+	Enucleation	–	–	–
18	69	M	Knee	Post. tib.	2×2×2	+	–	+	+	Enucleation	–	–	–
19	69	M	Ankle	Post. tib.	1.5×3×1	+	–	+	+	Enucleation	–	–	–
20	27	F	Leg	Peroneal	3×2×2	+	+	+	–	Enucleation	–	–	–
21	73	M	Leg	Post. tib.	2×5x3.5	+	+	+	+	Enucleation	–	–	–
22	57	M	Forearm	Radial	2×2×2	+	+	+	–	Enucleation	–	–	–
23	55	M	Leg	Peroneal	4.5×4×4	+	+	+	+	Enucleation	–	–	–
24	56	F	Foot	Digital	5×4×3	+	–	+	–	Enucleation	–	–	–
25	40	M	Leg	Post. tib.	3.7×4.4×3	+	+	+	+	Enucleation	–	–	–

br., Branch; pl., plexus; post., posterior; tib., tibial

Table 2. Imaging findings of the schwannoma series

Lesion	CT inhomogeneity	CT intensity	CT rim enhancement	MRI T1	MRI T2	MRI enhancement	Venous tumour stain	FDG-PET	FMT-PET
1	Homogeneous	Hypointense	+	>Muscle	Periphery>fat/central=fat	+	+	2.8	0.44
2	ND	ND	ND	<Muscle	>Fat	+	ND	0.7	0.78
3	ND	ND	ND	=	>Fat	+	ND	1.73	1.47
4	Homogeneous	Isointense	+	=	Periphery>fat/central=fat	ND	+	1.58	0.7
5	Homogeneous	Hypointense	+	<Muscle	>Fat	+	+	2.5	1.15
6	Homogeneous	Hypointense	–	=	>Fat	+	+	3.7	ND
7	Homogeneous	Isointense	+	=	>Fat	+	+	1.8	1.15
8	ND	ND	ND	=	>Fat	+		1.8	ND
9	ND	ND	ND	=	Periphery>fat/central=fat	ND	ND	1.93	ND
10	Homogeneous	Hypointense	–	=	Equal to fat	+	–	0.95	0.72
11	Homogeneous	Hypointense	–	=	≥Fat	+	–	0.95	0.75
12	Homogeneous	Hypointense	–	=	Periphery>fat/central=fat	+	–	0.96	0.9
13	Heterogeneous	Hyperintense	–	=	Equal to fat	+	–	1	1.07
14	Homogeneous	Isointense	+	=	Equal to fat	+	+	3.3	ND
15	Heterogeneous	Hyperintense	+	=	Periphery>fat/central=fat	+	–	1.67	1.23
16	ND	ND	ND	=	Periphery>Fat/Central=Fat	+	+	1	0.7
17	Homogeneous	Isointense	–	=	Equal to fat	+	–	1.2	0.55
18	Homogeneous	Isointense	–	=	Equal to fat	+	+	2.8	1.08
19	Homogeneous	Isointense	–	=	Equal to fat	+	+	1.79	0.93
20	ND	ND	ND	=	≥Fat	+	ND	0.33	ND
21	Heterogeneous	Isointense	+	=	Periphery>fat/central=fat	ND	+	ND	ND
22	ND	ND	ND	=	Periphery>fat/central=fat	+	ND	2.06	0.63
23	ND	ND	ND	=	>Fat	+	ND	ND	0.93
24	Homogeneous	Isointense	+	=	≥Fat	+	ND	2.38	ND
	ND	ND	ND	=	>Fat	+	ND	ND	ND

Results

Histopathological examination revealed all tumours to be schwannomas (with the classic Antoni A and Antoni B areas). Based on the clinical and imaging data, all tumours but one were treated by enucleation, after careful dissection from the nerve. Only one patient (lesion number 14), whose SUV on FDG-PET was 3.3 (unfortunately FMT was not performed), was treated by primary wide resection (Table 1).

The CT, MRI, DSA, FDG-PET and FMT-PET findings are summarised in Table 2.

PET findings

On visual assessment all 22 tumours examined by FDG-PET and the 17 examined by FMT-PET could be distinguished as areas of increased accumulation. Figure 1 demonstrates the representative cases. Ten out of 16 lesions evaluated by both FDG- and FMT-PET analyses showed low accumulation on both PET examinations (Fig. 1A). In contrast, four cases showed high accumulation of FDG, but all of these false-positive lesions revealed low accumulation of FMT (Fig. 1B). Quantitative values of both FDG- and FMT-PET are shown in Table 2. The SUVs for FDG ranged from 0.33 to 3.7, showing wide variation. Eight out of 22 lesions had SUVs in the malignant range as defined according to a previous study [13]. In contrast, SUVs for FMT ranged from 0.44 to 1.47; only two lesions had a value higher than 1.2, and were suspected to be malignant [16]. Among the lesions evaluated by both PET analyses, four showed high FDG SUVs. However, on visual assessment all of these false-positive lesions revealed low FMT SUVs, correctly indicating the lesions to be benign (Fig. 1B). There was no correlation between FDG and FMT SUVs in our schwannoma series (P=0.6104), suggesting a discrepancy between glucose metabolic activity and protein metabolism. The size of the tumours, as determined by gross examination of the specimen, ranged from 1×1×2 to 6×8.5×10 cm and showed a significant correlation with FDG SUVs (r=0.628, P=0.0013) (Fig. 2A), but not with FMT SUVs (r=–0.108, P=0.6849) (Fig. 2B).

CT findings

All 16 tumours examined by CT were clearly detected. There was variability in tumour homogeneity and enhancement pattern. Figure 3 demonstrates representative

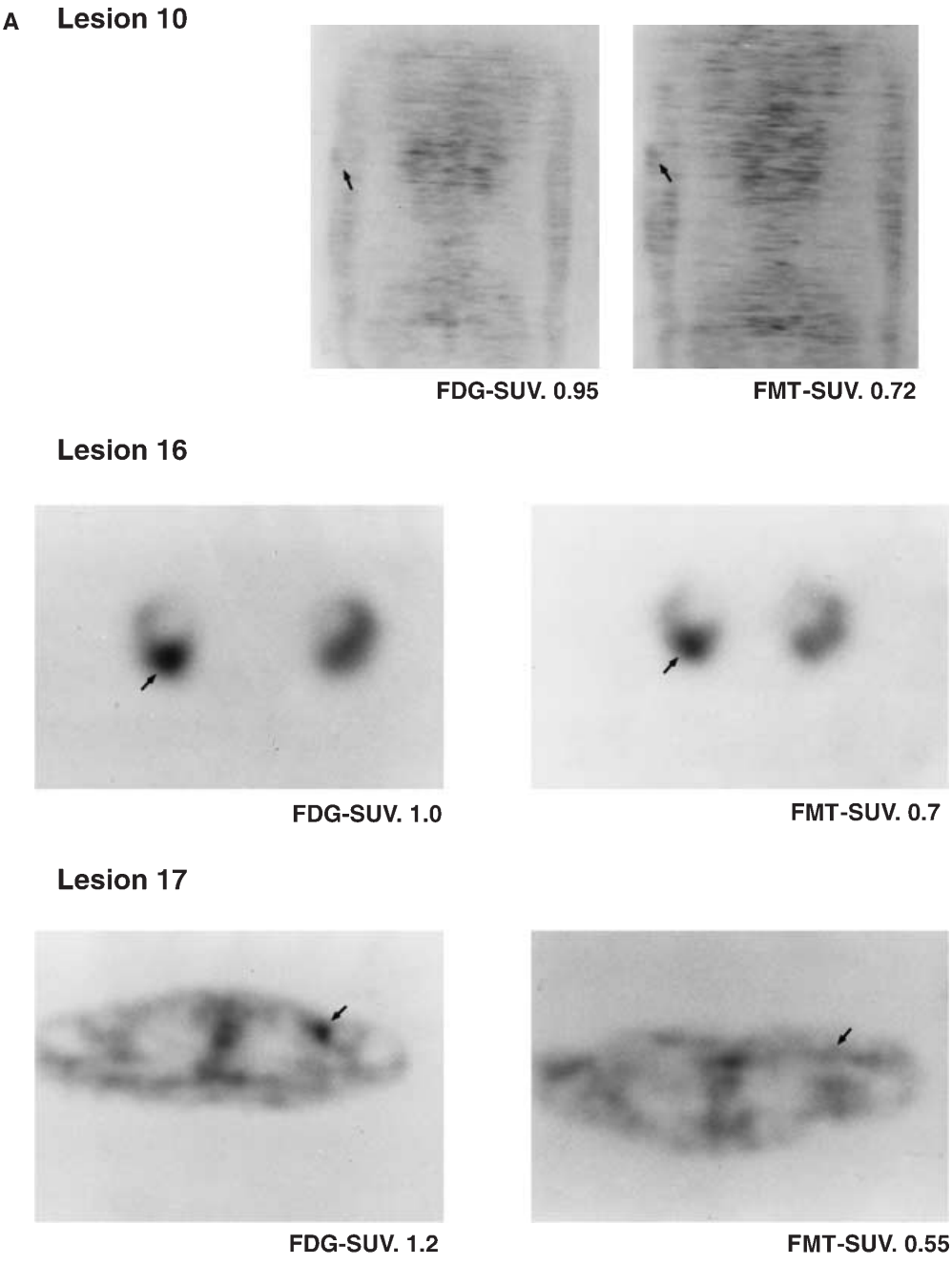

Fig. 1. PET images of three representative cases (lesions 10, 16 and 17) showing low accumulation of FDG (**A**), and three cases (lesions 1, 18 and 22) showing high accumulation (**B**). FMT accumulation is low in all lesions. SUVs are indicated in each image

CT images with (Fig. 3A) or without (Fig. 3B) rim enhancement. There was no statistically significant correlation of tumour homogeneity or enhancement with the intensity of either FDG or FMT uptake (Table 3).

MRI findings

MRI detected all 25 tumours. Twenty-four of the 25 tumours displayed a signal intensity the same as or slightly less than that of skeletal muscle on T1-weighted images, and all had a signal intensity similar to or greater than that of subcutaneous fat on T2-weighted images (Fig. 4). Only in the case of lesion 1 was tumour signal intensity on T1-weighted images greater than that of skeletal muscle (Fig. 4A). All 22 tumours examined showed uniform enhancement after injection of gadolinium (Fig. 4). Specific features of the internal architecture, such as a difference in signal intensity between the two histological compartments, were found on T2-weighted images, with the periphery showing a higher signal intensity than the central parts in eight tumours. Figure 4 shows three representative cases (lesions 1, 9 and 22) with such heterogeneous T2-weighted images (Fig. 4A) and two cases (lesions 5 and 11) with homogeneous images (Fig. 4B). There was no correlation between this heterogeneity and

Fig. 1B. Legend see page 1545

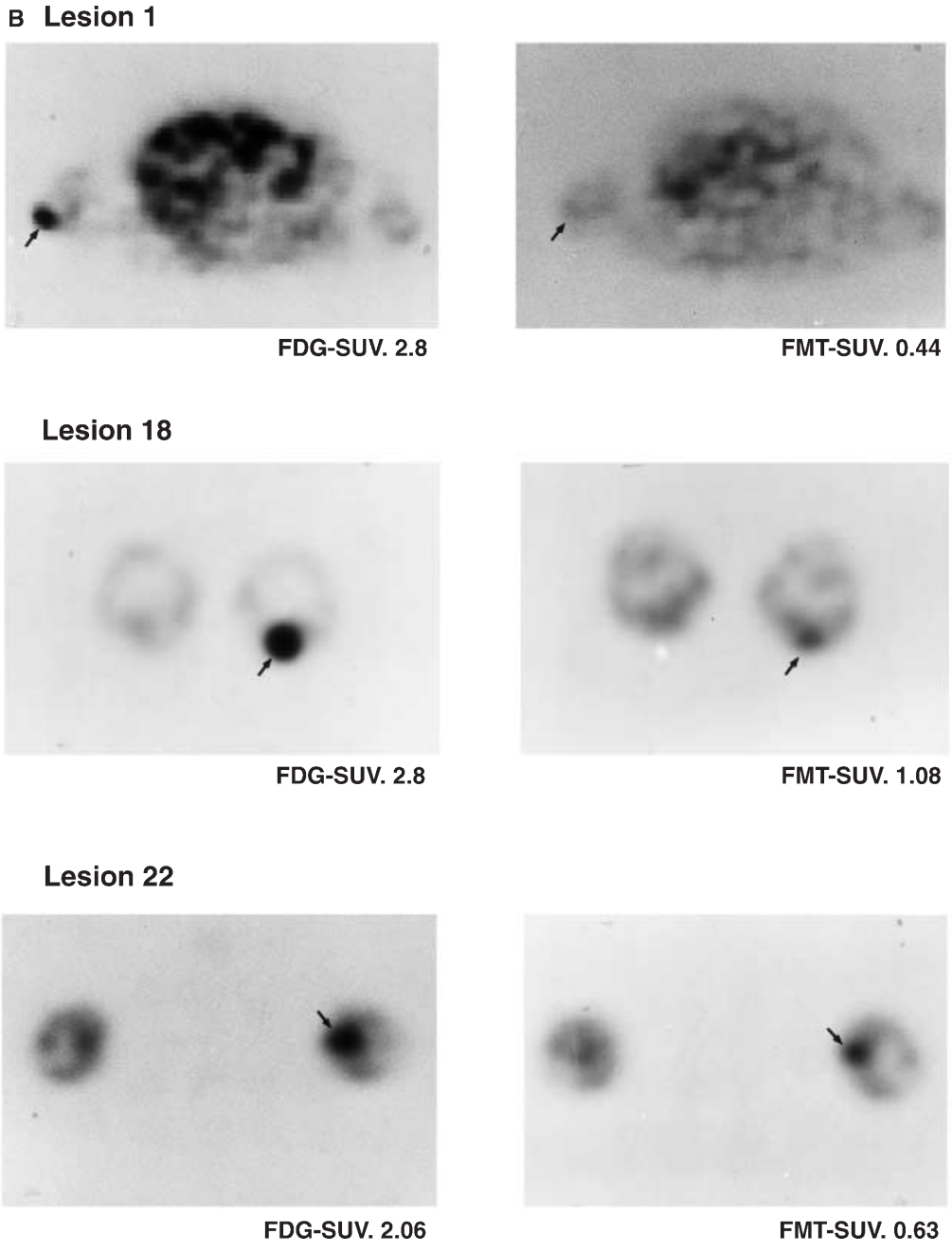

Fig. 2. Correlation of SUVs for FDG (**A**) and FMT (**B**) with tumour size

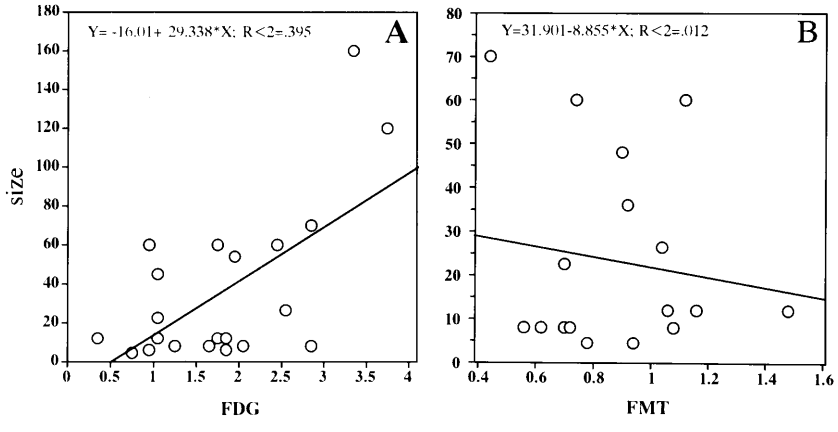

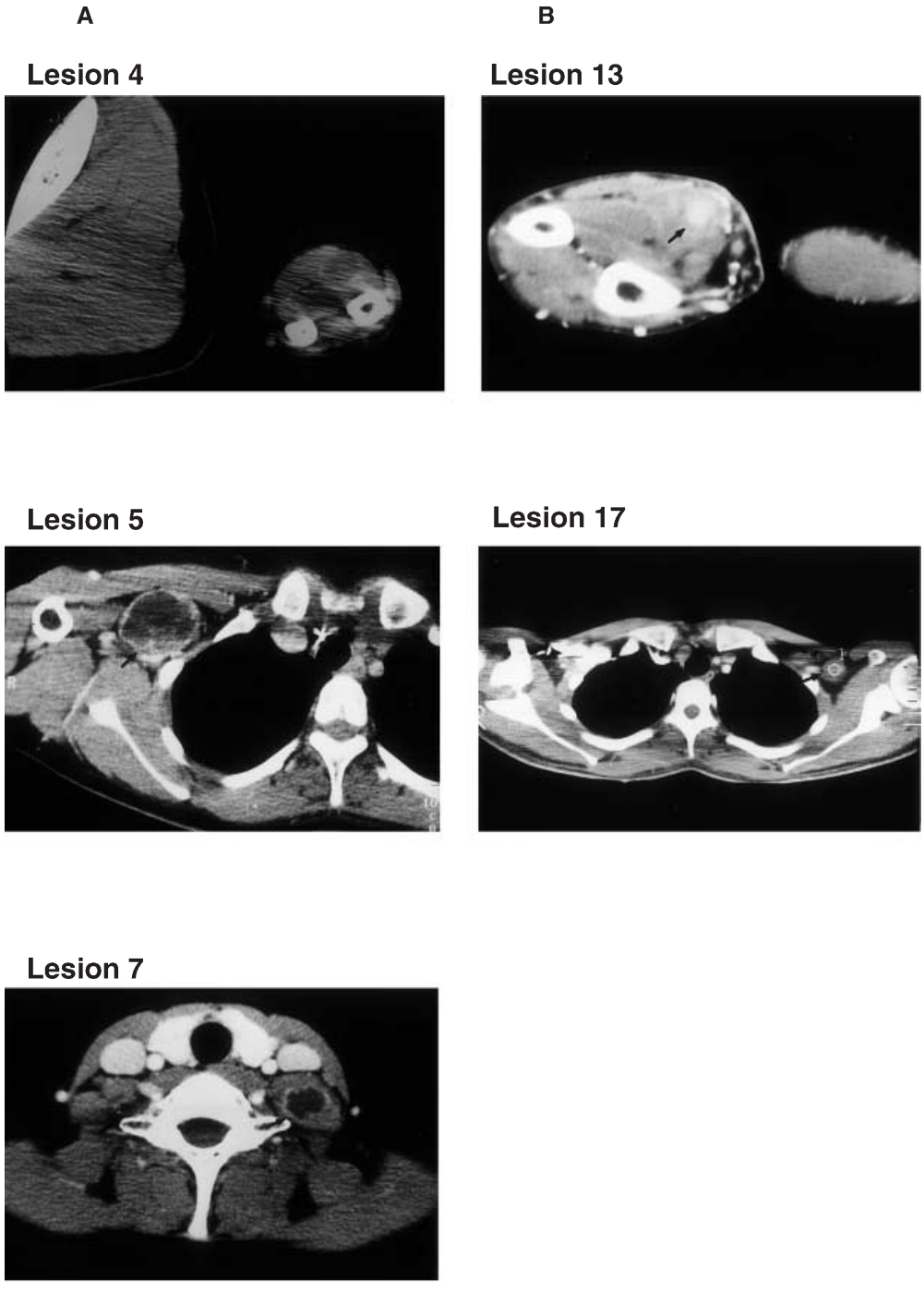

Fig. 3. Representative enhanced CT scans of three cases (lesions 4, 5 and 7) demonstrating rim enhancement (**A**) and two cases (lesions 13 and 17) showing homogeneous isointense tumour without rim enhancement (**B**)

FDG accumulation (mean, 1.71 and 1.80 for the positive and negative groups, respectively, P=0.8448) or FMT accumulation (mean, 0.77 and 0.96 for the positive and negative groups, respectively, P=0.1628).

DSA findings

Seventeen tumours were examined angiographically employing the criteria suggested by Abramowitz et al. [18]. Three tumours were moderately vascular; the remaining 14 tumours were mildly vascular with scattered small puddles of contrast material seen in the mid-arterial, capillary and venous phases. Multiple feeding vessels were noted in all lesions. No arteriovenous shunting or vascular encasement was identified. In addition, the presence of venous tumour staining was noted in some lesions, reflecting a high degree of vascularity of those lesions in the venous phase (Fig. 5). Regarding the vascularity and the presence of venous tumour staining, the tumours

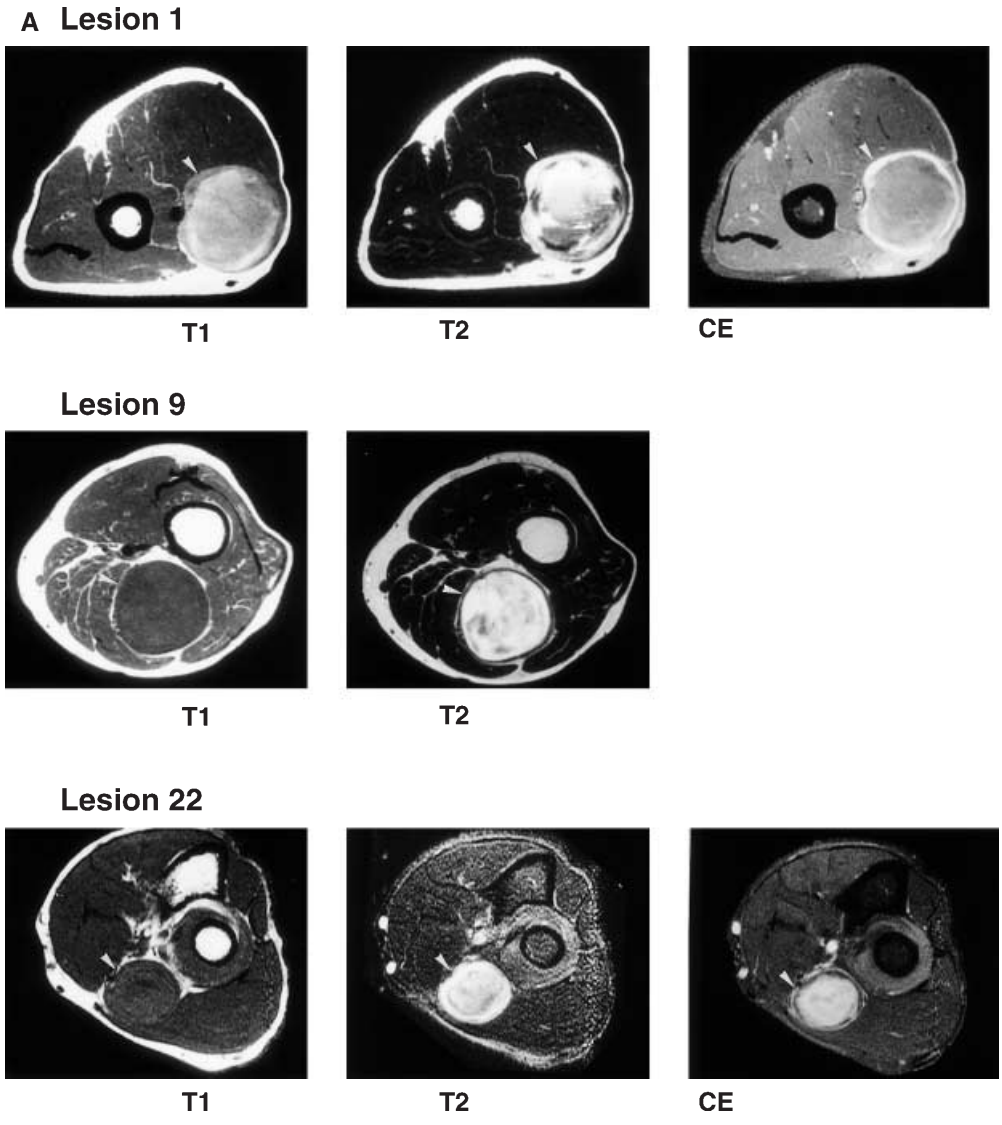

Fig. 4. T2-weighted MR images showing heterogeneous findings, which may correspond to internal histological architecture, in three cases (lesions 1, 9 and 22) (**A**), and homogeneous signals in two cases (lesions 5 and 11) (**B**). All lesions demonstrated uniform enhancement after injection of gadolinium. Lesion 1 was the only case with a signal intensity greater than that of skeletal muscle on T1-weighted images (**A**)

Table 3 Correlation of FDG and FMT SUVs with the imaging findings

Imaging findings		FDG SUV		FMT SUV	
Modality	Finding	Mean±SD	*P*[a]	Mean+SD	*P*[a]
CT	Homogeneous	2.06±0.93		0.84±0.25	
	Heterogeneous	1.34±0.47	0.3138	1.15±0.11	0.1186
	Rim enhancement (+)	2.29±0.64		0.93±0.35	
	Rim enhancement (–)	1.67±1.04	0.1960	0.86±0.19	0.6321
	Radio intensity				
	Isointense	2.12±0.71		0.88±0.25	
	Hyperintense	1.34±0.47	0.5026	1.15±0.11	0.1323
	Hypointense	1.98±1.19	0.7933	0.79±0.26	0.5946
MRI	T2 homogeneous	1.80±0.99		0.96±0.26	
	T2 heterogeneous	1.71±0.64	0.8448	0.77±0.27	0.1628
DSA	Venous tumour stain (+)	2.36±0.88		0.88±0.24	
	Venous tumour stain (–)	1.22±0.37	0.0062	0.87±0.25	0.9542

[a] Probability of no difference between the groups according to unpaired Student's *t* test

Fig. 4B. Legend see page 1548

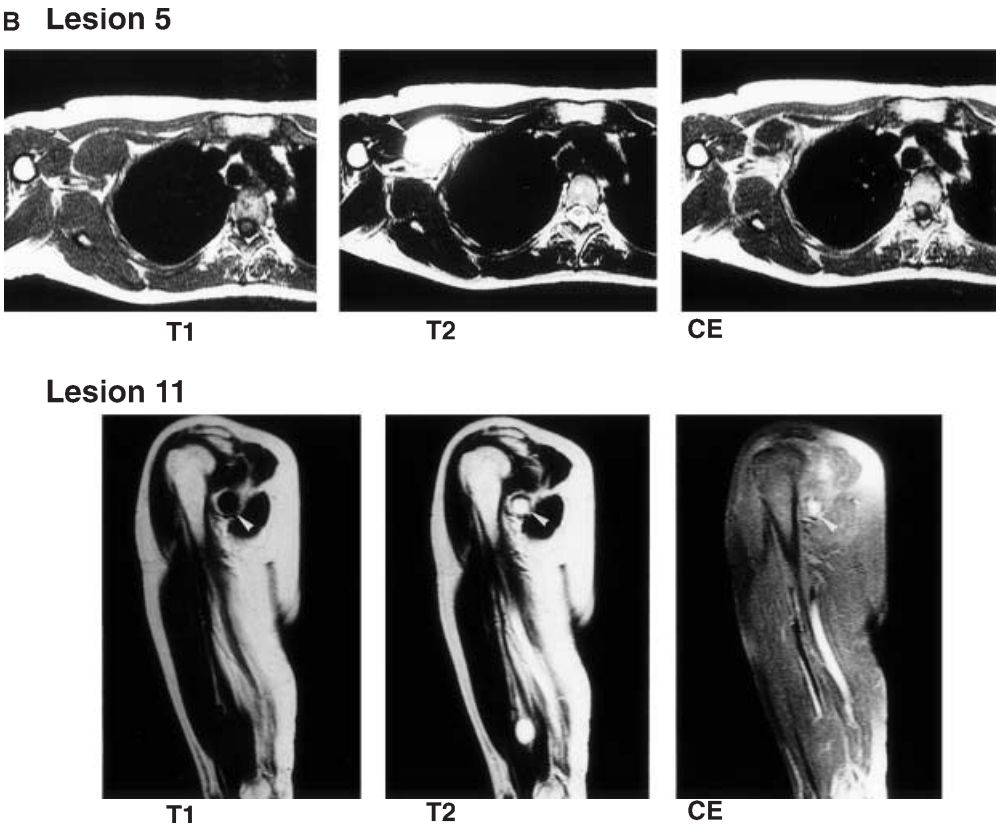

Fig. 5A, B. DSA. **A** A 40-year-old female patient (lesion number 8): note the absence of venous tumour staining in a left median nerve schwannoma (*arrow*) while a nearby lymph node shows some retention of stain (*small arrow*). **B** Positive venous tumour staining in a right ulnar nerve schwannoma (lesion number 6) (*arrow*)

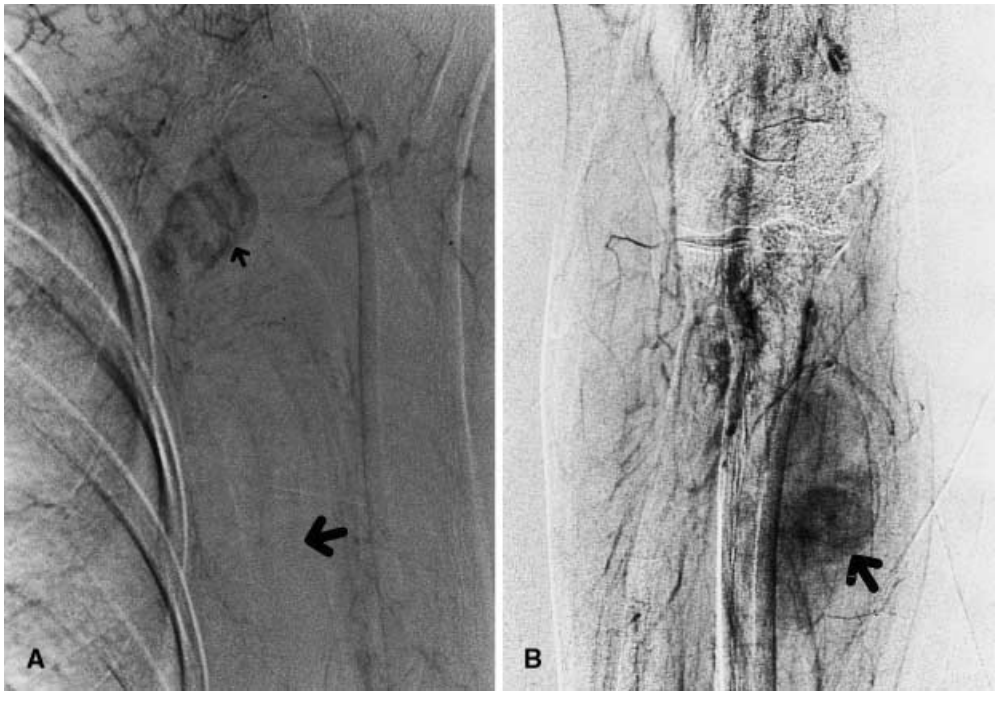

were divided into two groups, The mean SUV for FDG-PET of the venous tumour stain-positive group was 2.36, which was significantly higher than that of the negative group (1.22) (P=0.0062). In contrast, for FMT-PET no significant difference was found between the stain-positive and stain-negative groups with regard to the mean SUV (0.879 and 0.870 for the positive and negative groups, respectively, P=0.9542).

Postoperative findings

At the end of follow-up (ranging from 5 to 29 months with an average of 17 month), none of the patients had local spontaneous pain or tenderness. Only one patient (lesion number 11) had a positive Tinel's sign, while four patients had mild paraesthesia, which may have been due to postoperative perineural fibrosis, except in the patient whose tumour SUV was 3.3 (lesion number 14), who was treated by primary wide resection (Table 1).

Discussion

All of the schwannomas reported in our series were located on the flexor surfaces of the extremities. As already mentioned, 20 tumours presented with local pain and/or tenderness at the tumour site (80%), all but one produced local swelling (96%), and ten produced paraesthesia (40%). None of the patients had motor deficits, and 19 tumours (76%) elicited a positive Tinel's sign. These findings are consistent with those previously reported by Stout [3] and Kobayashi et al. [7]. In this series, 28% of this schwannomas originated from small sensory branches and 60% developed from large nerves (Table 1). Twenty percent of all schwannomas arose from the posterior tibial nerve.

Although CT, MRI and DSA permit tumour localisation and document useful anatomical details, none of these modalities provide specific criteria by which to distinguish benign schwannoma from malignancy [7, 22, 23, 24]. In the current series, imaging characteristics (Table 2) were relatively consistent on MRI. The internal architecture of cellular and myxoid components was most evident on T2-weighted MR images, which were characterised by relatively higher signal intensity at the periphery as compared with the centre of the tumours (Fig. 4).

High accumulation of FDG was found in eight cases (Fig. 1). Four out of them were analysed by FMT-PET, and all showed low accumulation (Fig. 1B). To confirm this qualitative evaluation, a semi-quantitative approach was also performed. Griffeth et al. demonstrated the average differential uptake ratio (DUR), a simple ratio of lesion to normal tissue FDG uptake, to be higher in malignant tumours than in benign lesions [12]. In our previous study, a highly significant difference in SUV, similar to that in the DUR, was demonstrated between benign and malignant musculoskeletal lesions [13]. However, when the cut-off value was set at 1.9, the specificity for correct diagnosis of malignancy was relatively low in spite of the high sensitivity, indicating that false-positive benign lesions were not neglected in FDG-PET [13]. It has also been suggested by Nieweg et al. that FDG is unsuitable for discriminating benign lesions from sarcomas with a relatively low malignancy grade [11]. In the present study, the SUV for FDG in schwannomas ranged from 0.33 to 3.7, showing wide variation. One-third of the lesions showed SUVs within the range indicative of malignancy. In fact, in one patient (lesion number 14) whose SUV on FDG-PET was 3.3, primary wide resection was performed, although schwannoma should normally be enucleated with careful dissection, especially when it originates from a large nerve. Fortunately only a minor sensory defect was left in the thigh of this patient. Even biopsies may present some risk. Using FDG as a PET tracer, eight tumours in our series showed an SUV within the range suggestive of malignancy (more than 1.9), indicating that FDG-PET may not be useful indicator for differentiation of schwannoma from malignant soft tissue sarcomas. Since SUV is operator and technique dependent, reliance on this semi-quantitative index presents a potential problem when it is used by other investigators with different instruments. Therefore the absolute value may vary in an institutional-dependent manner. However, the relative value may be useful, and most institutions might reach a similar cut-off value when a sufficiently large number of cases are considered. In fact, the SUV cut-off value for FDG of 1.9 [16] is very similar to the value of 2.0 reported by other institutions [25].

We demonstrated wide variation in the accumulation of FDG by schwannomas (0.33–3.7). Higher FDG SUVs correlated directly with increasing tumour size [17]. Larger schwannomas reportedly demonstrate frequent cystic changes and necrosis [1]. Of all the imaging characteristics evaluated in this study, including CT, MRI and DSA, we found that only positive venous tumour staining at DSA correlated significantly with the degree of FDG accumulation. This suggests that the SUV for FDG reflects the degree of tumour vascularity in schwannomas.

Our findings suggest that increasing tumour size results in relative ischaemia and hypoxia in schwannomas. This may induce neo-vascularisation, reflected as a positive tumour stain on DSA, and may accelerate anaerobic glycolysis, which leads to high FDG uptake [26, 27, 28, 29]. FMT accumulation showed no correlation with either FDG SUV or tumour size in this series. Since FMT is not metabolised through the glycolytic pathway [16], its accumulation may not be affected by hypoxia in larger tumours. This not only supports our hypothesis that increased FDG uptake may reflect the induction of neovascularisation by hypoxia in relatively larger schwannomas, but also suggests that FMT is less likely to yield false-positive results for malignancy in larger tumours.

In conclusion, if schwannoma is clinically suspected, CT, MRI and PET studies may be useful for detection and anatomical localisation. MRI apparently demonstrates the relative contribution of cellular and myxoid components as well as the degree of cystic degeneration and tumour necrosis. DSA is useful for pre-operative planning and findings correlate with the intensity of FDG uptake, reflecting the degree of tumour hypoxia and resultant neo-vascularity. Most importantly, FMT-PET may be most reliable modality for differentiating benign schwannoma from malignancy.

Acknowledgements. The authors thank Dr. Tomio Inoue and Dr. Takashi Yanagawa for their valuable help, and Mr. Oosawa for his assistance.

This work was supported in part by Grants-in-Aid for Scientific Research (C) 12671394 (H.W., K.T.), (C) 12671395 (H.W., T.S., K.T.) and (C) 13671489 (K.T., H.W., T.S.) from the Japanese Ministry of Education, Science, Sports and Culture.

References

1. Enzinger FM, Weiss SW. Benign tumors of the peripheral nerves. In: Enzinger FM, Weiss SW, eds. *Soft tissue tumors, 3rd edn.* St. Louis: Mosby, 1995.
2. Shinozaki T, Chigira M, Watanabe H, Arita S, Kanbe K. Multiple neurilemmoma in both legs. A case report. *Int Orthop* 1995; 19:60–62.
3. Stout AP. The peripheral manifestations of specific nerve sheath tumor [neurilemoma]. *Am J Cancer* 1935; 24:751–761.
4. Verstraete KL, Vander WoudeHJ, Hogendoorn PC, DeDeene Y, Kunnen M, Bloem JL. Dynamic contrast-enhanced MRI of musculoskeletal tumors: basic principles and clinical applications. *J Magn Reson Imaging* 1996; 5:311–321.
5. Pritchard DJ. Surgical management of common benign soft-tissue tumors. In: Simon MA, Springfield D, eds. *Surgery for bone and soft-tissue tumors, 1st edn.* Philadelphia: Lippincott-Raven, 1998.
6. Suh JS, Abenoza P, Galloway HR, Everson LI, Griffiths HJ. Peripheral (extracranial) nerve tumors: correlation of MRI and histologic findings. *Radiology* 1992; 183:341–346.
7. Kobayashi H, Kotoura Y, Sakahara H, et al. Schwannoma of the extremities: comparison of MRI and pentavalent technetium-99m-dimercaptosuccinic acid and gallium-67-citrate scintigraphy. *J Nucl Med* 1994; 35:1174–1178.
8. Lucas JD, O'Doherty MJ, Wong JCH, Bingham JB, Mckee PH, Fletcher CDM, Smith MA. Evaluation of fluorodeoxy glucose positron emission tomography in the management of soft tissue sarcomas. *J Bone Joint Surg [Br]* 1998; 80:441–447.
9. Adler LP, Blair HF, Makely JT, Williams RP, Joyce MJ, Leisure G, AL-Kaisi N, Miraldi F. Noninvasive grading of musculoskeletal tumors using PET. *J Nucl Med* 1991; 32: 1508–1512.
10. Kern KA, Brunetti A, Norton JA, Chang AE, Malawer M, Lack E, Finn RD, Rosenberg SA, Larson SM. Metabolic imaging of human extremity musculoskeletal tumors by PET. *J Nucl Med* 1988; 29:181–186.
11. Nieweg OE, Pruim J, Van Genkel RJ, Hoekstra HJ, Paans AMG, Molennar WM, Koops HS, Vaalburg W. Fluorine-18-flurodeoxyglucose PET imaging of soft tissue sarcoma. *J Nucl Med* 1996; 37:257–261.
12. Griffeth LK, Dehdashti F, McGuire AH, McGuire DJ, Perry D, Moerlein SM, Seigel BA. PET evaluation of soft tissue masses with fluorine-18 fluoro-2-deoxy-D-glucose. *Radiology* 1992; 182:185–194.
13. Watanabe H, Shinozaki T, Yanagawa T, Aoki J, Tokunaga M, Inoue T, Endo K, Mohara S, Takagishi K. Glucose metabolic analysis of musculoskeletal tumors using fluorine-18-FDG PET as an aid in preoperative planning. *J Bone Joint Surg [Br]* 2000; 82:760–767.
14. Tomiyoshi K, Amed K, Muhammad S, Higuchi T, Inoue T, Endo K, Yang D. Synthesis of isomers of ^{18}F-labelled amino acid radiopharmaceutical: position 2- and 3-L-18 F-alpha-methyltyrosine using a separation and purification system. *Nucl Med Commun* 1997; 18:169–175.
15. Inoue T, Shibasaki T, Oriuchi N, Aoyagi K, Tomiyoshi K, Amano S, Mikuni M, Ida I, Aoki J, Endo K. F-18 alpha-methyl tyrosine PET studies in patients with brain tumors. *J Nucl Med* 1999; 40:399–405.
16. Watanabe H, Inoue T, Shinozaki T, Yanagawa T, Oriuchi N, Ahmed AR, Aoki J, Tokunaga M, Takagishi K. PET imaging of musculoskeletal tumors with F-18 alpha-methyl tyrosine: comparison with F-18 fluorodeoxyglucose PET. *Eur J Nucl Med* 2000; 27:1509–1517.
17. Shah N, Sibtain A, Saunders MI, Townsend E, Wong WL. High FDG uptake in a schwannoma: a PET study. *J Comput Assist Tomogr* 2000; 24:55–56.
18. Abramowitz J, Dion JE, Jensen ME, Lones M, Duckwiler GR, Vinuela F, Bentson Jr. Angiographic diagnosis and management of head and neck schwannomas. *Am J Neuroradiol* 1991; 12:977–984.
19. Oriuchi N, Tomiyashi K, Inoue T, Ahmad K, Sarwar M, Tokunaga M, Suzuki H, Watanabe N, Hirano T, Horikoshi S, Shibasaki T, Tamara M, Endo K. Independent thalium-201 accumulation and fluorine-18-fluorodeoxyglucose metabolism in glioma. *J Nucl Med* 1996; 37:457–462.
20. Inoue T, Kim EE, Wong FCL,Yang DJ, Bassa P, Wong W-H, Korkmaz M, Tansey W, Hicks K, Podoloff DA. Comparison of fluorine-18-fluorodeoxyglucose and carbon-11-methionine PET in detection of malignant tumors. *J Nucl Med* 1996; 37:1472–1476.
21. Inoue T, Oriuchi N, Kunio M, Tomiyoshi K, Tomaru Y, Aoyagi K, Amano S, Suzuki H, Aoki J, Sato T, Endo K. Accuracy of standardized uptake value measured by simultaneous emission and transmission scanning in PET oncology. *Nucl Med Commun* 1999; 20:849–857.
22. Matsushita T, Takeda K, Tashiro T, Nakamura K, Nakagawa K, Katsuta K. Computed tomographic findings of peripheral type schwannoma; comparative study with histology. *Rinsho-Hoshasen* 1990; 35:1391–1395.
23. Cohen LM, Schwartz AM, Rockoff SD. Benign schwannomas: pathological bases for CT inhomogeneities. *Am J Roentgenol* 1986; 147:141–143.
24. Varma DGK, Moulopoulos A, Sara AS, Leeds N, Kumar R, Kim EE, Wallace S. MR Imaging of extracranial nerve sheath tumors. *J Comput Assist Tomogr* 1992; 16:448–453.
25. Dehdashti F, Siegel BA, Griffeth LK, Fusselman MJ, Trask DD, McGuire AH, McGuire DJ. Benign versus malignant intraosseous lesions: discrimination by means of PET with 2-[F-18] fluoro-2-deoxy-D-glucose. *Radiology* 1996; 200:243–247.
26. Haberkorn U, Ziegler SI, Oberdorfer F, Trojan H, Haag D, Peschke P, Berger MR, Altmann A, van Kaick G. FDG uptake, tumor proliferation and expression of glycolysis associated genes in animal tumor models. *Nucl Med Biol* 1994; 21:827–834.
27. Reske SN, Grillenberger KG, Glatting G, Port M, Hildbrandt M, Gansauge F, Berger H-G. Over expression of glucose transporter 1 and increased FDG uptake in pancreatic carcinoma. *J Nucl Med* 1997; 38:1344–1348.
28. Wahl RL. Targeting glucose transporters for tumor imaging: 'sweet' idea, 'sour' result. *J Nucl Med* 1996; 37:1038–1041.
29. Gallagher BM, Fowler JS, Gutterson NI, MacGregor RR, Wan CN, Wolf AP. Metabolic trapping as a principle of radiopharmaceutical design: some factors responsible for biodistribution of [^{18}F] 2-deoxy-2-fluoro-D-glucose. *J Nucl Med* 1978; 19:1154–1161.